Characterization and Behavior of Aluminum Foam Sandwich Fabricated by A Novel Approach Via Hot-Dip Process

Hu Zheng-Fei*, Yao Chen, Mo Fan

Shanghai Key Laboratory for R&D and Application of Metallic Functional Materials, School of Materials Science and Engineering, Tongji University, Shanghai 201804, China

*Corresponding author: E-mail: huzhengf@tongji.edu.cn; Tel: (+86) 2169585265

DOI: 10.5185/amlett.2020.051508

Metallurgical bonding aluminum foam sandwich (AFS) was fabricated by specially designed method of solder pre-coating via hot-dip and heat-press assisted with vibration. Peeling test and three-point bending test were performed to investigate the joints strength and flexural strength of the AFS. The results show that the joints have steady mechanical properties, and the joint fabricated with ultrasonic vibration has much higher peeling moment and flexural strength than that prepared only by hot-press. Microstructure observations of the joints indicate a good metallurgical bonding between Al face sheet and foam core was achieved. The seam of AFS fabricated by hot-press assisted with ultrasonic vibration looks more compact and the bonding interface fused together firmly. The bonding faces of aluminum sheet and foam core are obviously corroded by melt ZnAl alloy and an obvious interdiffusion took placed during hot-dip process and hot-press, so the chemical compositions in the diffusion transitional zone are continuous. However the seam of the AFS fabricated only by hot-press has visible macro-defects, and the worse is its bonding interface fused together partially, which severely degrades the bonding strength.

Introduction

Aluminum foam (AF) has unique mechanical and physical properties, possesses both characteristics of structural material and functional material. As a structural material, it has light weight and high mass/stiffness ratio; as a functional material, it owns unique physical properties of sound absorption, heat insulation, shock absorption, and electromagnetic shielding [**1-4**]. However, the low mechanical properties of AF limit its wide application. In order to enhance the performance of aluminum foam, it is usually used as core in sandwich structure, and the both sides are cladwith compact and stiff aluminum or other metal sheets. When the sandwich structures bear a great pressure or a stronger impact load, the two stiff face sheets carry axial load and offer sandwich structure bending and stretching capacity while the foam core bears shear load and supports the ability to undergo large deformation. As a lightweight composite structure, aluminum foam structure (AFS) maintains the characteristic of aluminum foam of function and lightweight, improves flexural stiffness and high-energy absorption capacity [**5-7**].

Various technologies have been proposed to fabricate sandwich structures with aluminum foam cores and dense face sheets. One of the most common and comparatively low-cost method to manufacture AFS is adhesive bonding, which combines cover sheet and AF core by polymeric adhesives [**1,8**]. Although the adhesive joint can stand the shear load, and can reduce the composite weight [**9,10**], there are still many problems of the adhesive bonding, such as the polymeric adhesives are difficult to recycle, the adhesive AFS cannot be used in high temperature conditions and the current high performance adhesives have given rise to considerable environment concerns [**11,12**]. Several techniques are proposed to fabricate metallic bonding AFS, such as friction stir incremental forming to transform a surface layer into a massive skin [**13**], laser foaming to produce the Al foam cores inside a hollow profile [**14**], rolling bonding and the powder metallurgy foaming process and self-propagating high-temperature synthesis (SHS) [**10**], roll-cladding the face sheets to foamable precursor materials and then foaming at a proper temperature to obtain the AFS [**15,16**]. AFS prepared by these techniques can achieve good metallurgical bonding but it is difficult to produce AFS with aluminum face sheets because the foaming temperature usually causes the aluminum face sheets to be melted [**17**]. AFS fabrication methods based on soldering orbrazing have been investigated and the main problem of these methods are the removal of the oxide film onthe bonding surfaces of the aluminum sheet and foam substrates, and development of suitable solder alloys with appropriate melting point and desirable wettability and fluidity. AlSi, SnZn and AlZn alloys are proposed as solder alloys to join Al-foam core with Al-sheet and

reliable bonding achieved by diffusion soldering [**18-24**]. However, Ashby *et al.*,[**8**] claim that soldering without flux requires at least partial removal of oxide films on bonding surfaces to allow molten solder alloy to directly contact the substrates. One prospective way to fabricate AFS is fluxless soldering and studies show that the AFS structure has reliable mechanical property [**22**]. In order to remove oxide film on the bonding surfaces, abrasive method have been introduced [**23,24**]. These investigations suggest that the bonding surface can be cleared by mechanical abrasion with appropriate tool under molten solder alloy. The solder is melted on bonding surfaces to form a coating by oxygen-propane torch, and then the metallic bonding is achieved by hot-press with vibration. These joining methods have presented some interesting metallic bonding solutions to fabricate AFS, however, no one clear exhibits obvious advantage for mass production of AFS components for practical application. In the interest of finding a way to fabricate AFS with low-cost and simple craft for large-scale products, there is still much work needed to do about proper process, suitable solder alloy and simple techniques to remove oxide film on aluminum and foam substrates to provide a joint the strength of which exceeds that of aluminum foam.

In current research works, ZnAl alloy is selected as the solder alloy for its moderate melting point, superior mechanical properties and excellent wettability [**25,26**]. It provides a novel method using hot-dip galvanizing to form ZnAl alloy pre-coating on the bonding surfaces of Al foam core and face sheet, then AFS structure is fabricated by hot-press assisted with vibration to combine the aluminum foam cores and face sheets. Peeling test and three-point bending test are performed to test bonding strength, and the interfacial microstructures are analyzed as well to investigate the joint strength mechanism. The results indicate that our AFS fabrication technology quite satisfies the requirement of sound metallurgical bonding and mass production of large-size AFS structures.

Experimental

Close-celled aluminum foam was used as core material, which was manufactured by the melt foaming process using TiH_2 as foaming agent in Sichuan Yuantaida Non-ferrous Corporation. The 0.41g/cm^3 density foam core was cut into 15mm in thickness. 1-mm-thick 5056 aluminum alloy sheet was selected as face sheets. An alloy Zn-10Al was selected as solder. The ZnAl binary-phase diagram shows the solidus and liquidus temperature of Zn-10Al are 380.0℃ and 426.5℃. Solidus temperature is the minimum temperature for liquid-solid diffusion interactions to occur, and the liquidus temperature indicates the good capillary flow can take place, so the wide liquidus to solidus temperature range indicates the ability to joint larger clearancesor make it possible to fabricate large size AFS structure.

Before soldering, the bonding surfaces of Al foam core and face sheets were pretreated in the following steps: (1) chemically polishing in 10% NaOH solution 1min and rinsing in running water immediately for 2min, then drying by air blower, (2) the bonding surfaces of aluminum foams and face sheets were immersed in the melting bath of Zn-10Al alloy melted at 430-450℃ for 1min, then homogeneous ZnAl coating on the bonding surfaces of aluminum foams and face sheets was obtained. After hot-plating, The pre-coating surfaces of Al foam core and face sheets were stacked in the configuration shown in **Fig. 1(a)**, then underwent the soldering process in a thermo-compressor as the heat-platform preheated at 450℃ with a pressure of 0.1 MPa in a thermo-compressor heated at 450℃about 5min. During that time, the ZnAl coating on bonding surfaces would remelt together to form fusion seam. Holding the pressure until the fusion seam solidified when heating stopped, then AFS structure was obtained, and in this case AFS structure named as HP for short. In order to gain a solidified fusion seam, another case of AFS structure was fabricated assisted with ultrasonic vibration (HPUV) during hot-press. The ultrasonic vibration works at a frequency of 20 kHz and 1 kW in power. The samples prepared for peeling test, only one face sheet was bonding to the foam core.

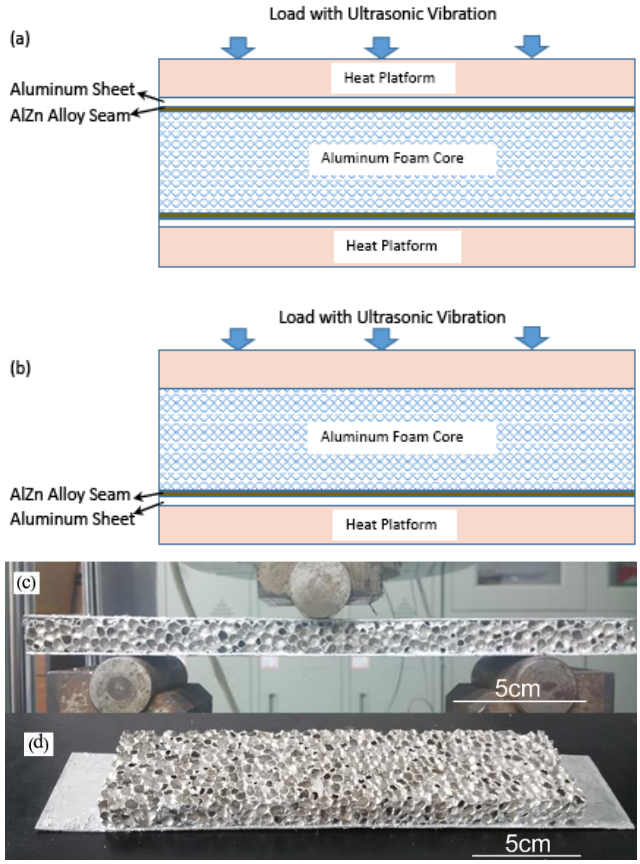

Fig. 1. (a) Schematic drawing of fabrication ABS by hot-press assisted with vibration, (b) one side bonding for peeling test. The pictures of samples for three-point bending test(c), and standard peeling test (d).

AFS structures werepreprepared in the sizes of 240mm×50mm for three-point bending testand one side bonding face sheet structure in the size of 300mm×50mm

for peeling test. Three-point bending test is performed in a universal mechanical test machine (MTS 800) with a load speed of 6mm/min and support span of 200mm. The three-point bending test assembly consisted of three cylindrical steel rollers with 20 mm diameter and 200 mm span length as shown in **Fig. 1(c)**. In this study, the test stopping condition was set when the load began to decrease to half of the maximum or the sample cracked visibly or face sheet debonded, loading was stopped.

According to the recommendations of the ASTM C393 standards, the test specimens have a rectangular cross section and the geometric parameters are given above. The actual test set-up with installed specimen is shown in **Fig.1(c)**. The drum-peeling tests according to ASTM D-1781 were conducted with a constant load speed of 25mm/min. Specimen for the peeling tests is also shown in **Fig. 1(d)**. Both tests were carried out on a series of five samples.

The bonding interfacial characterization of AFS wasobserved by Optical Microscope (OM, Olympus GX51) and Scanning Electron Microscope (SEM, FEI Nova Nano SEM 450) equipped with an energy dispersive X-ray spectrometer (EDS).

Results and discussion

Three-point bending test

Fig. 2(a) shows three-point bending load-deflection curves of aluminum foam (AF) and AFS samples of HPUV and HP, here HPUV and HP are marked for AFS fabricated with or without UV assistance respectively. The three curves are all composed of three sections, an initial elastic deformation section, the followed plastic deformation section and the final failure section. Compared with the AF curve, HPUV and HP curves show much stronger flexural strengths and can undergo much more deformation. This is mainly due to the fact that the aluminum face sheets of the sandwich structures can contribute significantly to the flexural properties. Compared HP with HPUV, the curves of load-cross head deflection for both samples in **Fig. 2** show obvious liner elastic behavior for both samples and almost overlap. Both curves show that their elastic behaviors range at the beginning 1.8 and 2.4mm deflections within loads of 1200N and 2300N respectively. Beyond the elastic loads, curves in **Fig. 2** also show that the specimens start to deform plastically with different behaviors for different samples. It can be seen that the bending strength of HPUV is about 35% higher than that of HP with 60% longer plateau plastic deformation section in deflection. With the deflection increasing, an abrupt load loss occurred at the deflection of about 15.0 mm for HP. **Fig. 2(c)** displays the load decrease dramatically due to debonding between face sheet and foam core because of shear failure. For HPUV, load loss rapidly at the deflection around 25.0mm can be seen in **Fig. 2(b)**. **Fig. 2(d)** shows that the failure of HPUV is due to crack growth under the load indenter and no visible debonding can be seen. The longer plateau of plastic formation means the HPUV structure has much higher energy absorbing ability.

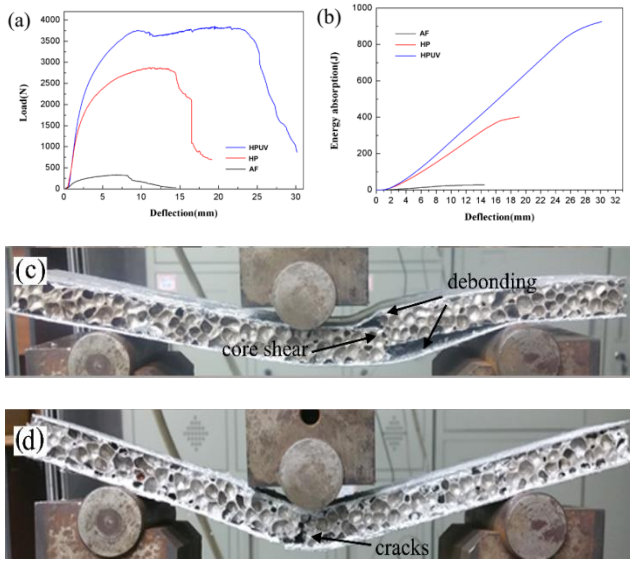

Fig. 2. Three-point properties of aluminum foam and AFS, (a) load-deflection curves, (b) energy absorption. The typical failure appearances of three-point bending samples (c) HP and (d) HPUV.

Table 1. Results of three-point bending test and peeling test.

Skin material and thickness (mm)	density of AF Core (g/cm3)	Joining method	Bending strength (kN)	Energy absorption (J)	Peeling moment (N.mm/mm)
Al-5056 /1.0	0.4	HP	2.8±0.4	380±50	40±10
		HPUV	3.8±0.7	900±190	100±15

Table 1 gives the three-point bending test results. The average bending strength of HPUV is 3850N, which is much higher than that of HP of 2850N. This resultis obviously due to the bonding strength between face sheets and foam core and the higher bonding strength enhances the AFS stiffness obviously. **Fig. 3(b)** shows the energy absorbing capability of AFS of HP and HPUV. It is evident that the energy absorbing capability of HPUV is also much higher than that of HP. Since good interfacial bonding between foam core and face sheet is the prerequisite for a better mechanical response of the AFS structures, it can be concluded that a better metallurgical bonding between AF core and face sheets in HPUV is realized.

Bonding strength in AFS

The peeling moments of AFS fabricated with different techniques are also given in **Table 1**. The average peeling strength of HPUV is 99 N.mm/mm, which is much higher than HP with an average peeling strength 40N.mm/mm. **Fig. 3(a)** shows the appearances of samples after peeling test. **Fig. 3(b)** shows the detailed appearances in **Fig. 3(a)** marked by squares.

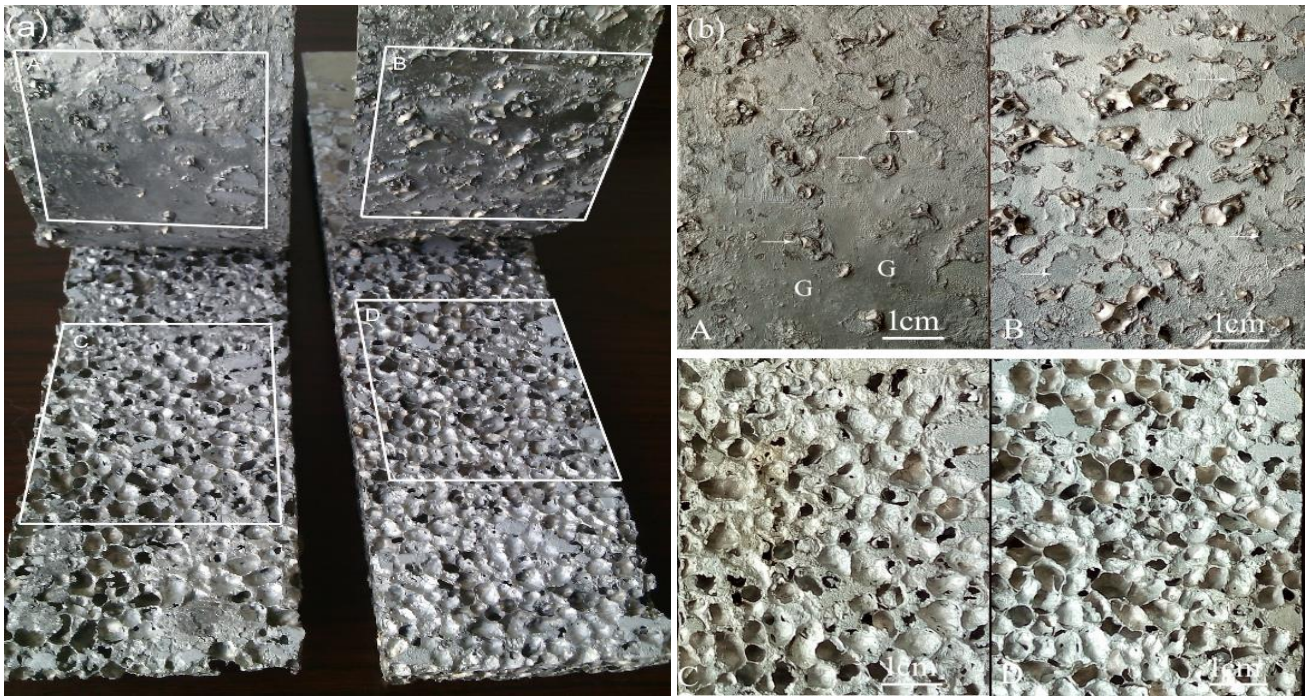

Fig. 3. Appearances of peeling test samples, (a) prepared by hot-press (left) and ultrasonic vibration (right), and (b) corresponding detailed appearances in the area of black boxes in (a).

Fig. 3 displays the characteristics of peeled surfaces. First, some pieces of foam were torn off from foam and adhered to the aluminum sheets, which indicates where the bonding strength between substrates of aluminum sheet and foam core is strongerthan the foam core; Second, the ZnAl coating was not split away from the both substrates, which means the pre-coating is well bonded with the substrates. It also can be seen in **Fig. 3(b)-A,** few pieces of aluminum foam wells adhered to the split face sheetin HP sample, which means the main clearage path is in the bonding interface. On the split face Al sheet in **Fig. 3(b)-A,** some areas as indicated by arrows show there the solder partly split away and adhered to the corresponding foam core surface and where the spherical caps of foam cell are covered by solder. Furthermore, the areas marked by letter G on the split surface are glossy, and the opposite cell caps on foam surface are still covered with coating, but the coating surface is not as smooth as the pre-coating, which is beruffled and sunken into cell caps slightly. It might be related to the air sealed in caps shrinking while cooling down. These features imply where the pre-coating on the foam surface re-melted but the pre-coating on both substrates did not fuse together during hot-press. The jointing interface is partly metallurgical fused together and the apparent fusion area is around 1/3, so the bonding strength for HP sample is lower and generally peeling failure is due to tear along the bonding interface. However, much more pieces of foam wall to be torn off in HPUV sample as showing in **Fig. 3(b)-B**, and most parts of the split surface of aluminum sheet were adhered with pieces of aluminum foam well, so the aluminum sheet is well bonded with foam core. There are also few areas as indicated by arrows the solder splitaway and adhered to the corresponding foam core surface and covered the cell caps. Apparently the jointing interface of HPUV sample is mostly metallurgical fused together and the apparent fusion area is above 2/3. The peeling test of HPUV sample shows that its peeling moment is much higher than that of the HP, and the Al cover sheet was split mostly across the foam core, so its bonding strength is greater than that of the foam core.

It can be deduced from above that the failure mode of the peeling tests of both samples of HP and HPUV is different, the sample HP failed mainly in the combined boundary and the sample HPUV mainly across the Al foam core, which is obviously related to the bonding strength whether the bonding faces fused together. The peeling strength of sandwich structure of HPUV sample is twice as much as HP, which manifests that the hot-dip coating and hot-press with ultrasonic vibration is an effective way to fabricate a sound metallurgical bonding sandwich structure. However HP structure shows a low bonding strength, so just hot-press is not reliable for practical application [**18**].

Jointing characteristics

The Optical Microscope images of the cross-section bonding seams of the AFS fabricated from two different ways showing in **Fig. 4(a)** and **Fig. 4(b)**. The well bonding interface shows that not only foam well sections on the AF surface are bonded with the seam but a great part of the foam cell spherical caps on the AF surface are also bonded with the seam because they are partly filled with ZnAl solder. This appearance significantly increases

the interface fusion area to enhance the bonding strength. However, as shown in **Fig. 4(a)** and **Fig. 4(b)**, the bonding seam of HPUV is continuous and compact while that in HP contains macro-defects such as gas pores in seam and cracks along the surface of cell wall. These macro-defects obviously affect the interface effective fusion area and deteriorate the bonding strength.

Generally, the bonding seam is eutectic ZnAl alloy, which contains a physical mixture of two phases of α-Al andη-Zn. The ZnAl binary-phase diagram indicates that Al and Zn do not form intermetallic phase. The eutectic point for AlZn system is 380.0℃ and at this temperature the liquid (Zn+Al) solidifies and transforms into Al-rich α phase and Zn-rich η-phase (hcp) eutectoid. While cooling, unstable supersaturated α-Al phase and η-Zn phase further decompose into α-Al phase (fcc) and η-Zn phase, so the OM images in **Fig. 4** shows some lamellar eutectic.

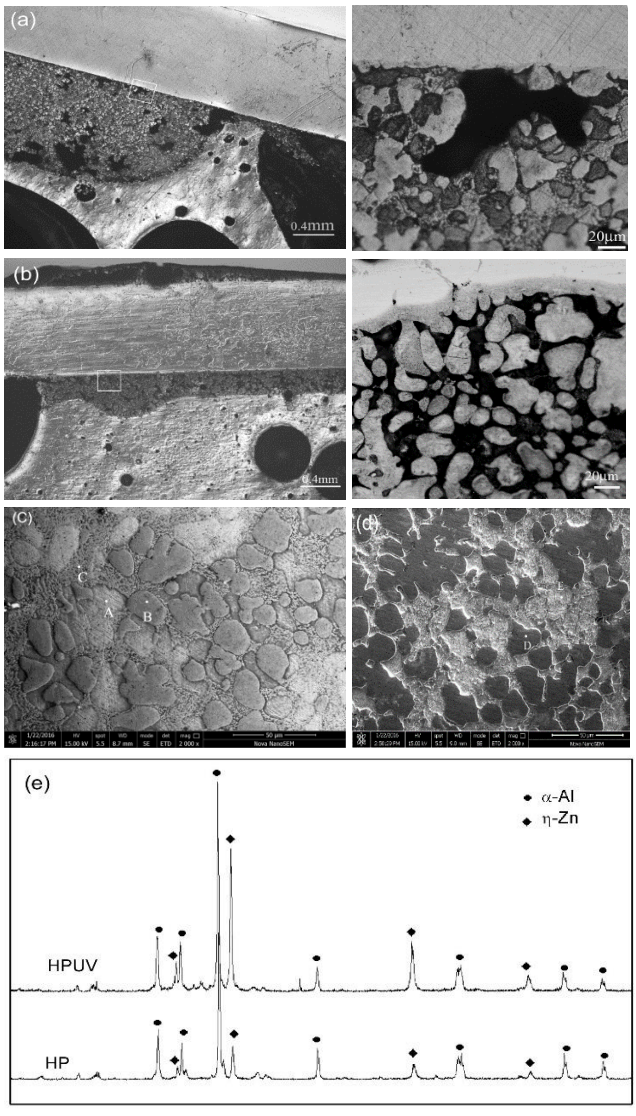

Fig. 4. Optical microscope images of typical bonding seams in samples prepared by (a) HP and (b) HPUV and inserts, corresponding SEM images of the bonding seams of (c) HP and (d) HPUV, (e) XRD patterns of the bonding seams of HPUV (above) and HP (below).

The cross-section bonding seams were further observed by Scanning Electron Microscope. SEM images in **Fig. 4(c)** and **Fig. 4(d)** display the fusion seams in two structures. The constitutive phases of the fusion seams can be divided roughly according to their microstructure morphologies. The fusion seam in HP has three different phase zones in appearance can be seen in **Fig. 4(c)** marked with A, B and C and the fusion seam in HPUV has two phase structures marked with D and E in **Fig. 4(d)**. Corresponding spot EDS analysis was employed to detect the different chemical compositions of these different phase structures. Three spectra were collected in each single phase zone and an average EDS analysis results are given in **Table 2**. A and B are Al and Zn rich phases respectively. Engaged with the chemical compositions and ZnAl binary phase diagram, it can be identified that phase A is α-Al and phase B is η-Zn. Combined with the image feature of lamellar and chemical composition between α-Al and η-Zn, C should be α-Al/η-Zn eutectoid. The results of EDS spot analysis at D and E are also given in **Table 2**. It can be deduced that D and E are α-Al and η-Zn respectively. **Fig. 4(e)** is XRD diffraction diagrams of fusion seams of the two AFS structures and the peaks in the profile are indexed as α-Al or η-Zn. It clearly indicates that no additional phase can be found in both samples and this result is consistent with above analysis.

Table 2. Element compositions and phase structure of the spots marked in Fig. 4(c) and (d).

Spots	Elements (at%)		
	Al	Zn	phase
A	62.65	37.35	α-Al
B	20.96	79.04	η-Zn
C	42.55	57.45	α-Al/η-Zn
D	71.13	28.87	α-Al
E	24.88	75.12	η-Zn

The above results indicate that the AFS fabricating process obviously affects the interface microstructure. HPUV soldering with ultrasonic vibration has a relative integrated eutectic microstructure close to equilibrium microstructure. However, HP soldering has a quasi-eutectic microstructure, and it could be decomposed further at suitable condition. So the vibration enhances the eutectic reaction.

Fig. 4(a) and **Fig. 4(b)** also show that the joint interface between solder and substrates of Al sheet or foam core displays a good wettability and obvious dendrites can be seen in the seam close to the substrates. The formation of dendrites close to the substrates should be related to the high temperature gradient for the high thermal conductivity of substrates. Furthermore, to compare with the seams observed by SEM Back-Scattered Electron (SEM-BES) images in **Fig. 5(a)** and **Fig. 5(b)**, the appearance of the dendrites clear show that the seam close to the interfaces contains more α-Al phase or Al element, which should be related to the liquid (Zn+Al) solidified firstly close to substrates and transformed into α-Al and Zn-rich η phase eutectoid. SEM-BES images present the atomic number contrast to discriminate

between particles when they have special chemical compositions. As shown in **Fig. 5**, the grain boundaries of the substrates of AF and Al sheet close to the seam are visible with distinct black-white contrast, which implies that Zn atoms have diffused into substrates deeply and the grain boundaries serve as diffusion tunnels. So the bonding surfaces of substrates are apt to etch in melted ZnAl alloy, and the main elements of Al and Zn atoms interdiffusion led to the chemical compositions in gradient distribution across the bonding interfaces.

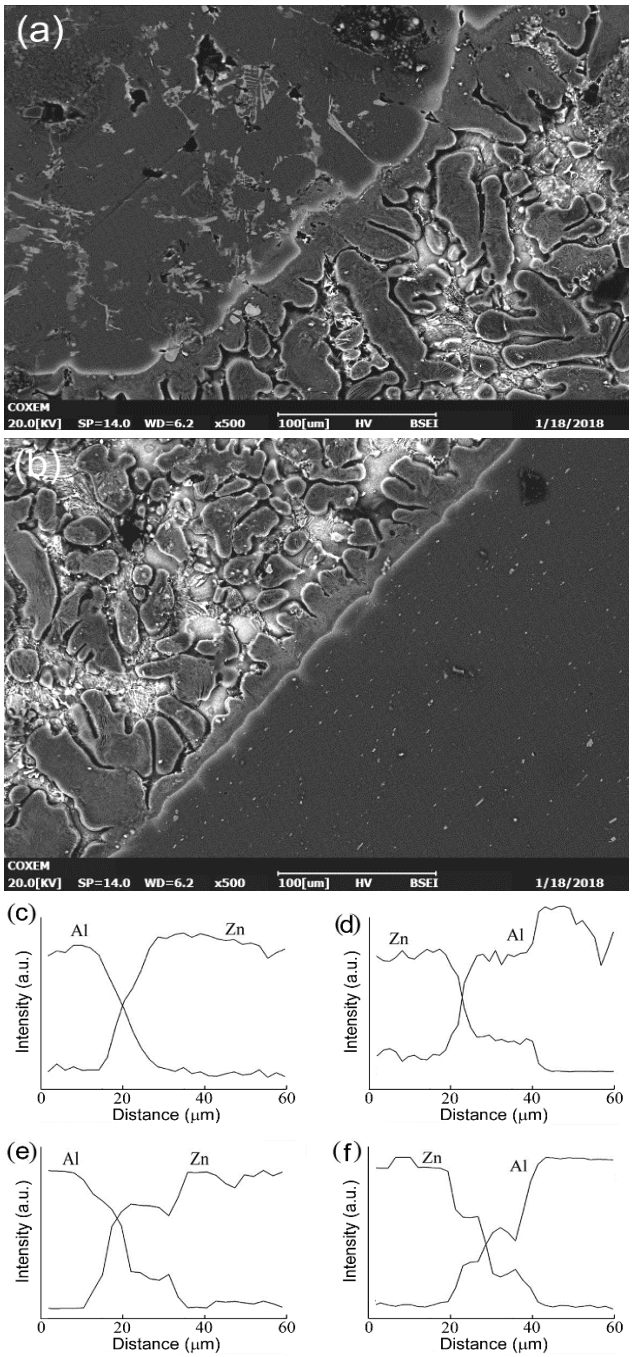

Fig. 5. SEM-BSE images of at seam interface between (a) foam core and (b) sheet in HPUV sample, (c) to (f) are EDS line-scanning analysis results of Al face sheet to solder alloy or solder alloy to foam core in HPUV and HP samples.

The mechanical properties of Zn-10Al alloy are much superior to those of foam core. The fusion seam made of Zn-10Al alloy in HPUV is continuous and compact, thus in peeling tests, the fracture location was mainly in aluminum foams. Otherwise, the peeling fracture in HP mainly failed in bonding seam because there were macro-defects in seam.

The EDS line-scanning analysis was performed to examine the chemical elements distribution across the interfaces and the results are displayed in **Fig. 5(c)** to **Fig. 5 (f)**. It is clear that the zinc and aluminum elements were distributed continuously through the interfaces of ZnAl solder and substrates, which means that a mutual diffusion was realized in both fabricated ways. As a main and high soluble element in Al alloy, Zn atom has relative low active diffusion energy and high diffusivity, which promote the interface fusion formation. The continuous distribution of alloy elements across interfaces should contribute to the sound bonding between solder and substrates, which also indicates that good wetting between solder and substrates was obtained and well metallurgical bonding was achieved.

Furthermore, as shown in **Fig. 5(a)** and **Fig. 5(b)**, the bonding interface lost their straight alignment and turned into zig-zag, which implies that the original smooth faces of substrates were eroded and dense pits formed during hot-dip coating and further eroded during hot-press with vibration, which means the surface layer of substrates was fused with solder alloy during hot-dip coating and hot-press.

Discussion

In this study, Zn-10Al alloy is selected as solder for its excellent wettability to aluminum substrates of aluminum sheet and foam core, and which can be illustrated by the phase relationship between zinc and aluminum [**22**]. In previous studies [**27,28**], solder alloys were specially designed with complex composition to improve their wettability and fluidity. The high mutual solubility of elements contributes to the wettability to the substrates, but depresses fluidity. In this study, the solder alloy is first coated on substrates of Al sheet and foam core by immersing them in molten ZnAl alloy bath, and then bonded by hot-press, so in this case, only the solder wettability need to be considered. That is why a binary alloy with composition of 90 wt% Zn-10wt% Al was chosen as the solder.

In the fabricating process, the bonding faces of Al face sheet and foam core were first polished, and then immersed in ZnAl melting bath. When fresh substrates immersed in ZnAl melting bath, the thin oxide film formed shortly on substrate surfaces can be destroyed mostly by the melting ZnAl alloy, and the zinc-based solder coating with good wettability to aluminum substrates is obtained. However, as shown in **Fig. 3**, cracks between the interface of the fusion seam and aluminum foam indicates that the hot-dip coating cannot achieve complete wetting on substrate surface. As shown

in Fig. 4(a), the seam contains some macroscopic defects which formed during hot-press process when seam resolidified. These defects obviously weaken the strength of the seam and affect the bonding strength.

The characteristics of the bonding interfaces in **Fig. 5** reveal the sound bonding are formed relative to the Zn atom diffusion from ZnAl coating into the substrates as well as Al diffusion in opposite direction. Element Zn is a typical alloying component for Al alloys and its solubility is the highest among other alloying elements [**29**]. During hot-dip coating process, the thin oxide film on the bonding faces is easy destroyed by reaction with abundant Zn atoms in liquid Zn-10Al alloy. With Zn atoms diffused into the substrates, especially at grain boundaries close to the substrate surfaces, the concentration of Zn element would increase enough high and lead to melting due to the melting point of Al alloy decreases dramatically with Zn content increased. With diffusion proceeding, surface grains partly melted and the melting grain boundaries widened due to the strong capillary effect [**30**]. As shown in **Fig. 6**, the oxide film can be destroyed further by continuous liquid phase forming at the substrate surface, which would float and break the thin oxide film, so the ZnAl alloy displays well wet to the substrates of aluminum sheet and foam core.

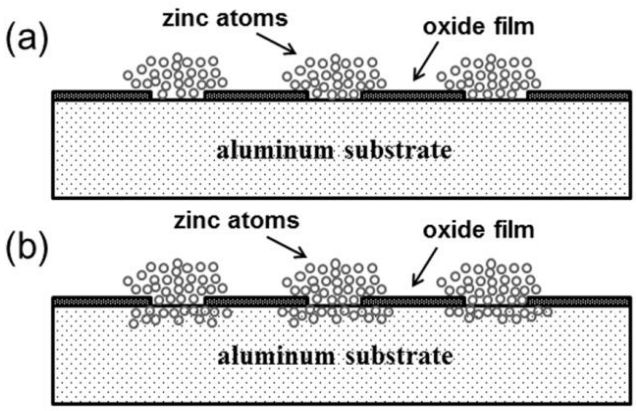

Fig. 6. Schematic process of oxide film removing, (a) before inter-diffusion, (b) after inter-diffusion.

Past studies show that the ultrasonic vibration can contribute to wetting mainly due to the induced cavitation effect **[8,24,31,32]**. During the combining process assisted with ultrasonic vibration and hot-press, cavitation effect can be generated. The cavitation-induced mechanical effects (such as jets, shockwaves and acoustic streaming) [**33,34**] can disrupt the oxide film further, therefore much fully wetting can be achieved. The ultrasonic vibration can also contribute to the exclusion of gas in the liquid phase due to the mechanical stirring effects induced by cavitation effect [**24**]. This can be confirmed by the fact that no gas pores can be observed in the seam shown **Fig.4(b)**, while obvious gas pores emerged in HP sample showing **Fig.4(a)**. Without vibration, the oxide film was disrupted partly and the rest part finally retained along the interface between the fusion seam and the substrates. Because of the oxide film is bad wet to solder alloy, so cracks formed along the interface as shown in HP sample showing in Fig. 3.

Generally, the HPUV joint shows much comprehensive bonding, due to the ultrasonic assisted fabrication method compacts the bonding interface and refines its microstructure. Effect of ultrasonic vibration on grain refinement has been widely reported [**8,22,35,36**] and ultrasonic treatment induces refinement and changes morphology of the fusion seam. Compared **Fig. 4(c)** and **Fig. 4(d)**, grain refined slightly in the fusion seam of HPUV, it is clear shown that no obvious α-Al/η-Zn eutectoid dendrites in HPUV seam, which means the ultrasonic vibration refines the dendrite or decomposes it. In fact, the ultrasonic vibration refines grain by dendrite fragmentation and enhances nucleation [**22,25,37-42**]. The most striking feature of the HPUV seam is no macroscopic defects of pores or cracks in the fusion seam and interfaces. So the ultrasonic vibration changed the morphology of the fusion seam obviously. The dendrites fragmentation is caused by mechanical effects of the ultrasonic-induced cavitation effects, which can disrupt the dendrites and prevent the formation of pores and cracks since the cavitation effects collapse these macroscopic defects. The fragments of the disrupted dendrites can act as the solidification sites and offer more opportunities for nucleation, then microstructure would be refined. In this study, the hot-press temperature is around 450℃, which is approximately 25℃ higher than the melting point of Zn-10Al alloy. The nuclei induced by the ultrasonic vibration hardly exists in the over-heated melt once the ultrasonic vibration stopped, so no obvious refined eutectoid microstructure can be seen in the HPUV bonding seam, but it really refines the dendrites in the seam and compacts it as well.

Conclusion

AFS was fabricated by specially designed pre-coating of solder ZnAl alloy by the hot-dip process and hot-press assisted with ultrasonic vibration. Well metallurgy bonding between aluminum face sheet and foam core was obtained. Major conclusions can be summarized as follows:

The hot-dipping process produces continuous and firm pre-coating of ZnAl alloy on the substrates of aluminum sheet and foam core. The oxide film on substrates can be effectively removed by liquid/solid interdiffusion and interface migration.

AFS fabricated by hot-press assisted with ultrasonic vibration has much higher peeling moment and much more superior flexural properties than that fabricated just by hot-press. So the former is torn mainly across the foam core and the latter mainly along the combined boundary.

The former jointing interface is mostly metallurgic ally fused and its apparent fusion area is twice the latter. So the ultrasonic vibration assistance well excludes the gas in the melting solder, which obviously improves the AFS interface fusion and enhances the bonding strength.

An obvious interdiffusion took place during fabrication process and led to a continuous composition distribution across the bonding interface, which should contribute to the sound bonding between solder and substrates. So the hot-dip pre-coating and hot-press assisted with ultrasonic vibration is an effective way to fabricate a sound metallurgical bonding sandwich structure. Pre-coating of ZnAl alloy via hot-dip on substrates of Aluminum sheet and foam core as solder is a practical way for AFS mass fabrication.

Acknowledgement

This work is supported by the National Key Research and Development Program of China (2017YFB0103700) and the National Science Foundation of China (51971163).

Keywords

Aluminum foam sandwich; hot-dip pre-coating, bonding strength, seam interface, interdiffusion.

Received: 12 January 2020
Revised: 29 February 2020
Accepted: 13 March 2020

Author biography

Prof. Zheng-Fei Hu is a senior professor in School of Materials Scinece and Engineering Tongji University. Prof. Hu has been working in the field of metallurgy physics, and he also focuses on the development and application of new lightweight alloy materials with significant engineering background. Most research programs involve in experimental studies of structure-property relations, including the effect of microstructural evolution, phase transformations and interface structure attribute on mechanical or physical performances.

References

1. Gbison, J.; Ashby, M. F.; Cellular Solids: Structure and Properties; Cambridge University Press, UK, **1997**.
2. Davies, G. J.; Zhen, S.; *J. Mater. Sci*., **1983**, *18*, 1899.
3. Levine, B.; *Adv. Eng. Mater*., **2008**, *9*, 788.
4. Banhart, J.; *Prog. Mater. Sci.*, **2001**, *46*, 559.
5. Kapil, M.; Yip, T. H.; Sridhar, I.; Hong, P. S.; *Mater. Sci. Eng. A*, **2005**, *409*, 292.
6. Harte, A. M.; Fleck, N. A.; *Adv. Eng. Mater.*, **2000**, *2*, 219.
7. Ruan, D.; Lu, G. X.; Yat, C. W.; *Comps. Struct.*, **2010**, *92*, 2039.
8. Ashby, M. F.; Evans, A. G.; Fleck, N. A.; Hutchinson, J. W.; Metal Foams: A Design Guide; Butterworth-Heinemann, Boston, USA, **2000**.
9. Adderley, C. S.; *Mater. Des.*, **1988**, *9*, 287.
10. Hao, Q. X.; Qiu, S. W.; Hu, Y. B.; *J. Rare Metal. Mater. Eng.*, **2015**, *44*, 548.
11. Nabavi, A.; Khaki, J.; Vahdati; *Sand. Struct. Mater. J.*, **2011**, *13*, 177.
12. Barnes, T. A.; Pashby, I.R.; *J. Mater. Process. Technol.*, **2000**, *99*, 72.
13. Matsumoto, R.; Tsuruoka, H.; Otsu, M.; *J. Mater. Process. Technol.*, **2015**, *218*, 23.
14. Campana, G.; Ascari, A.; Fortunato, A. L.; *Opt. Laser Technol.*, **2013**, *48*, 331.
15. Baumgartner, F.; Duarte, I.; Banhart. J.; *Adv. Eng. Mater.*, **2000**, *2*, 168.
16. Zhao, H.; Elnasri, I.; Girard, Y.; *Int. J. Impact Eng*., **2007**, *34*, 1246.
17. Neugebauer, R.; Lies C, Hohlfeld, J.; Hipke, T.; *Prod. Eng.*, **2007**, *1*, 271.
18. Nannan, C.; Yi, F.; Jie, C.; Bin, L.; Fanyan, C.; Jingsong, Z.; *J. Rare Met. Mater. Eng.*, **2013**, *42*, 1118.
19. Kitazono, K.; Kitajima, A.; Sato, E.; Matsushita, J.; Kuribayashi, K.; *Mater. Sci. Eng. A*, **2002**, *327*, 128.
20. Huang, Y. X.; Gong, J.; Lv, S. X.; Leng, J. S.; Li, Y.; *J. Sci. Technol. Weld. Join.*, **2012**, *17*, 636.
21. Sedliakova, N.; Simancik, F.; Kovacik, J.; Minar, P.; Proc. Metallschaume Conf. on Metal Foams; Banhart, J. (Ed.); MIT Publication, USA, **1997**, pp177-85.
22. Huang, Y.; Gong, J.; Lv, S.; Leng, J.; Li, Y.; *Mater. Sci. Eng. A*, **2012**, *552*, 283.
23. Shirzadi, A. A.; Kocak, M.; Wallach, E.R.; *J. Sci. Technol. Weld. Join.*, **2004**, *9*, 277.
24. Wang, H.; Yang, D.; He, S.; Feng, J.; *J. Alloys Comp*., **2016**, *671*, 346.
25. Yang, J. L.; Xue, S. B.; Peng, X.; *Mater. Sci.Eng. A*, **2016**, *651*, 425.
26. Ji, F.; Xue, S. B.; Lou, J. Y.; *Trans. Nonfer. Met. Soc. China*, **2012**, *22*, 281.
27. Wang, H.; Yang, D.; He, S.; Feng, J.; *J. Mater.Sci. Technol.*, **2010**, *26*, 423.
28. Wan, L.; Huang, Y.; Lv, S.; Feng, J., *Comp. Struct.*, **2015**, *123*, 366.
29. Zhu, Y. H.; *Mater. Trans.*, **2004**, *45*, 3083.
30. Mendez, P. F.; Rice, C. S.; Brown, S. B.; *Weld. J.*, **2002**, *81*, 181S.
31. Das, A.; Kotadia, H. R.; *Mater. Chem. Phys.*, **2011**, *125*, 853.
32. Xu, Z. W.; Yan, J. C.; Zhang, B. Y.; Kong, X. L.; Yang, S.Q.; *Mater. Sci. Eng. A*, **2006**, *415*, 80.
33. Zhang, S.; Zhao, Y.; Cheng, X.; Chen, G.; Dai, Q.; *J. Alloy Compd.*, **2009**, *470*, 168.
34. Rozenberg, L. D.; Physical principles of ultrasonic technology; Springer, Boston, MA, USA, **1973**.
35. Xiao, Y.; Ji, H.; Li, M.; Kim, J.; Kim, H.; *Mater. Des.*, **2013**, *47*, 717.
36. Xu, Z.; Ma, L.; Yan, J.; Chen, W.; Yang, S.; *Mater. Chem. Phys.*, **2014**, *148*, 824.
37. Atamanenko, T. V.; Eskin, D. G.; Zhang, L.; Katgerman, L.; *Metall. Mater. Trans. A*, **2010**, *41*, 2056.
38. Changle, D. M. C.; *Acta Metall. Sin*., **2010**, *46*, 885.
39. Swallowe, G. M.; Field, J. E.; Rees, C. S.; Duckworth, A.; *Acta Metall*., **1989**, *37*, 961.
40. Zhang, L.; Wu, G. H.; Wang, S. H.; Ding, W. J.; *Trans. Nonfer. Metal. Soc. China*, **2012**, *22*, 2357.
41. Ramirez, A.; Qian, M.; Davis, B.; Wilks, T.; StJohn, D. H.; *Scri. Mater*., **2008**, *59*, 19.
42. Jian, X., Xu, H.; Meek, T. T.; Han, Q.; *Mater. Lett.*, **2005**, *59*, 190.